

# Measurements of Controllable Pitch Propeller Blade loads Under Cavitating Conditions

Stuart Jessup<sup>1</sup>, Martin Donnelly<sup>1</sup>, Ian McClintock<sup>1</sup>, Scott Carpenter<sup>1</sup>

<sup>1</sup> Naval Surface Warfare Center Carderock Division, West Bethesda, Maryland

## ABSTRACT

To improve the prediction of the alternating blade loading under real operating conditions, a test program was conducted to measure the alternating blade forces in inclined flow in a water tunnel where effects of cavitation could be assessed. For these tests, an in-hub blade dynamometer was used along with a downstream slip ring housing. Instantaneous load variations were also measured to quantify peak transient loads due to cavity collapse. Loading excitation due to strut wake turbulence was also identified. The measured inflow was used to compare load predictions to the measured results.

## KEYWORDS

Propellers, Cavitation, Loads, Blades, Dynamometers

## 1 INTRODUCTION

In the 1970's the advent of large controllable pitch propellers brought on structural problems with the blade attachment bolts and hub components. This led to a model and full scale test program to determine the alternating blade loads produced by the nonuniform propeller inflow under various operating conditions for open shaft and v-strut hull forms. Tests by Boswell (1978) determined the alternating blade loads in steady ahead conditions, including seaway effects of hull pitching and regular waves. Since then, using this data for validation, computational predictive tools<sup>2</sup> have been refined to predict the alternating loads. Cavitation effects have been ignored in predicting design loads based on the assumption that cavitation will reduce the peak loads. Over the years it has been hypothesized that cavitation reduced the blade load periodic variation since the low pressure on the blade surface would be limited by vapor pressure. Since little data has been available to quantify these effects, simple load computations have been made assuming computed pressure distributions are truncated at vapor pressure.

Increases in load could occur due to collapse of cavitation on the blade, which may not be periodic in nature, and may phase average out of the bin average data acquisition process utilized for this test.

The objective of this paper was to help answer some of these questions.

## 2 WATER TUNNEL TEST DESCRIPTION

Tests were conducted in 2004 in the NSWCCD 36" water tunnel. The open jet test section was used with an inclined shaft configuration similar to previous tests of propellers utilizing a shaft barrel, v struts and an open shaft. A single blade dynamometer was installed inside the hub of propeller model 4990 which utilized removable blades in the hub. The propeller in the tunnel required a slip ring assembly attached downstream of the hub, as shown in Figure 1. The effect of the assembly presents some computational modeling difficulty, but was required, since wiring upstream was prohibited due to the CV universal joint of the inclined shaft hardware. Figure 2 shows the exploded view of the hub, with the dynamometer designed to measure primarily blade spindle torque, but also blade thrust, and blade side force with limited sensitivity.

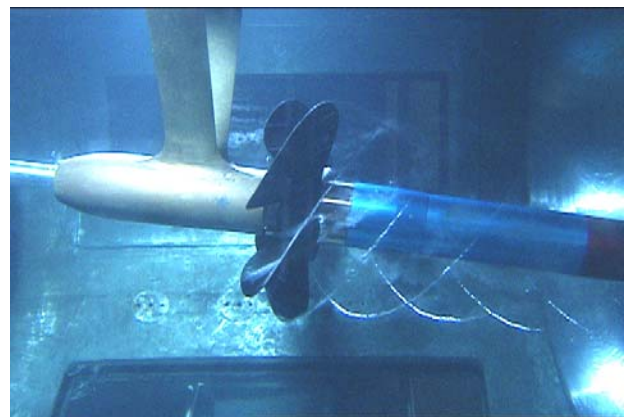


Figure 1. Propeller 4990 in the 36inWT under cavitating conditions.

## 3 PROPELLER AND DYNAMOMETRY

Propeller 4990 is 15.857"(402.77cm) diameter(D), five bladed controllable pitch propeller model. The propeller has removable blades, which were adapted to a new designed hub, which was split to accommodate a cylindrical type, strain gage dynamometer. Cavitation tests were conducted on this model by Jessup (1993). Propeller model 4990 utilizes a standard NACA type blade section which produces leading edge cavitation at high speeds.



**Figure 2. Exploded view of propeller hub**

Figure 3 shows the strain gage dynamometer used in the test with its primary purpose to measure the blade spindle torque, (the torque about the center axis of the rotation of the controllable pitch blade). With the desire to obtain additional information, the sensor was also gaged to measure side forces to provide blade thrust and blade side force. These channels had less sensitivity and also some problems with varying interactions. The cause was due to placement of the semiconductor strain gages too close to the clamping inner end of the flexure. When the blades were changed out and the hub was re-clamped, sensitivities changed, requiring interaction calibrations after every blade change out. Thrust data will be presented, but large DC bias corrections were made to align the mean blade thrust results with data using the measured shaft thrust.

Calibrations were conducted accounting for interactions amongst the two side forces and the axial moment channels. The interactions were applied during data acquisition. The uncertainty of the load measurements and the associated tunnel parameters are shown in Table 1.

**Table 1. Test parameters and errors**

Parameter	Units	±Error
Spindle torque, $M_y$	in-lbs	14
Blade thrust, $F_x$ (Pos fwd)	lbs	11
Blade side force, $F_z$	lbs	15
Tunnel Velocity, $V$ ( $\Delta P$ )	ft/sec	0.2
Propeller rps, $n$	rps	0.2
Shaft thrust, $T$	lbs	5
Shaft torque, $Q$	ft-lbs	2
Tunnel static pressure, $P_0$	psi	0.2

Air spins results, shown in Figure 5, produced an effect on spindle torque,  $M_y$ , which was approximately 20% below predictions from an analysis code which utilized an integration of blade mass. Details of the blade fillets were excluded. Error shown places some uncertainty on the centrifugal load corrections.

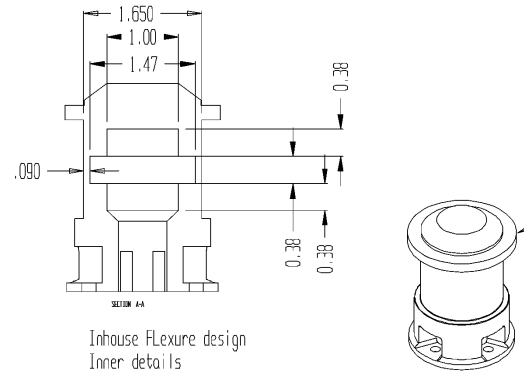


**Figure 3. Propeller blade load dynamometer (dimensions in inches)**

Corrections were also made to the measured loads to account for centrifugal effects due to blade weight. This was performed by spinning the prop in air in the water filled tunnel. Since the shaft bearings could not be operated in air, an air spin test box was built around the propeller, and pumped with air to permit spinning the propeller in air in the tunnel, as shown in Figure 4.



**Figure 4. Air spin test box**

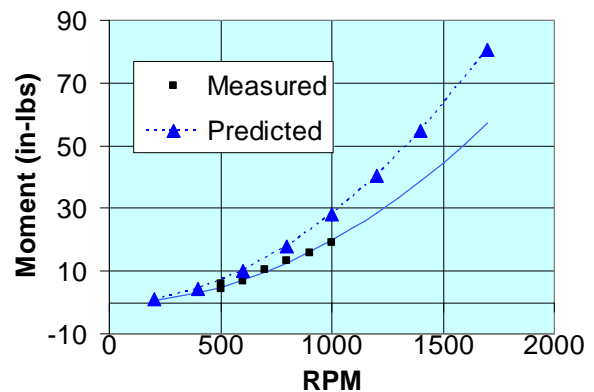


**Figure 5. Spindle torque,  $M_y$  air spin results**

#### 4 TEST CONDITIONS

Test conditions were drawn up to cover a range of advance coefficients,  $J = V/nD$ , and cavitation conditions from large scale high speed conditions to noncavitating

conditions. This range of conditions is shown in Table 2. The propeller was operated within its operating J range at design pitch. It were also operated at its trail shaft condition where one propeller drives the ship and the other propeller trails, or free wheels. This condition was performed at a pitch setting above the design pitch setting. The test condition ranges are tabulated below. Trail shaft data is not included in this paper.

**Table 2. Range of test conditions for P4990**

Rpm	J V/nD	V ft/sec	P psia
556 - 1700	0.8 - 2.8	17 - 43.3	11-31

### 5 Water Tunnel Propeller Inflow Wake

The propeller inflow wake is a simulation of an open shaft, v strut, shaft barrel configuration. The shaft inclination is adjustable to match the flow inclination determined from tow tank wake survey the hull and Froude scaled free surface. The universal joint provides a wake which somewhat resembles the wake of the shaft on the real configuration. A wake survey is shown in Figure 6 Further discussion of DTMB's water tunnel surveys for this configuration was reported by Jessup (1993). The effective inflow angle for the set-up was 8.9 degrees.

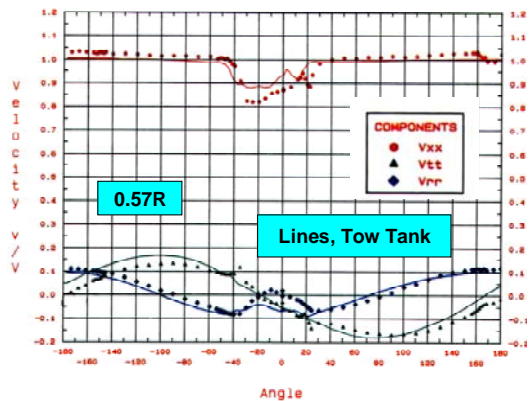


**Figure 6. Propeller inflow wake survey at 0.57R**

### 6 DATA ACQUISITION

Data acquisition was performed using LabVIEW version 7.1 to record the data channels listed in Table 1. Data was sampled at 2000 Hz including the shaft angular position from an absolute positioning encoder with a resolution of 0.04 degrees. After a 10 second data collect sequence, load data was sorted into 256 angular bins from the measured encoder position taken simultaneously with the force measurements. Data was averaged and bin rms values were determined. Blade weight was accounted for by slowly rotating the propeller, collecting data, then fitting a once per revolution sine wave to the variation with rotation. The amplitude and phase of the sine wave represented the weight of the blade and the location of the reference position of the blade relative to

gravity. The blade weight was removed from the periodic loading from the blade dynamometer.

### 7 TEST RESULTS - EFFECTS OF CAVITATION ON LOADS

Initial results in Figure 7a show the effect of reduction in tunnel pressure and the onset of extensive cavitation on the alternating blade spindle torque. Figure 7b shows a similar plot for the blade thrust, Fx. Cavitation extent at the tunnel static pressure of 14 and 18 psi (absolute) is shown in Figure 8. Extensive leading edge cavitation at the high blade load region, around 100 degrees blade position, results in reduction in leading edge loading and spindle torque.

Oscillatory behavior can be seen in the phase averaged periodic loads, which become more pronounced with the introduction of cavitation. Videos with stroboscopic illumination showed cavity length oscillations which may have been real time phase averaged cavity dynamic behavior. The oscillations could also be associated with blade vibration.

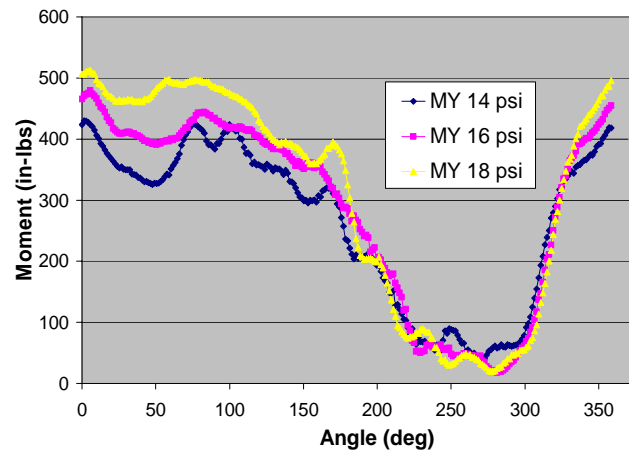


**Figure 7a. Variation of Blade Spindle Torque, My, with blade angle at varying tunnel pressures, 1698 rpm, J=1.12**

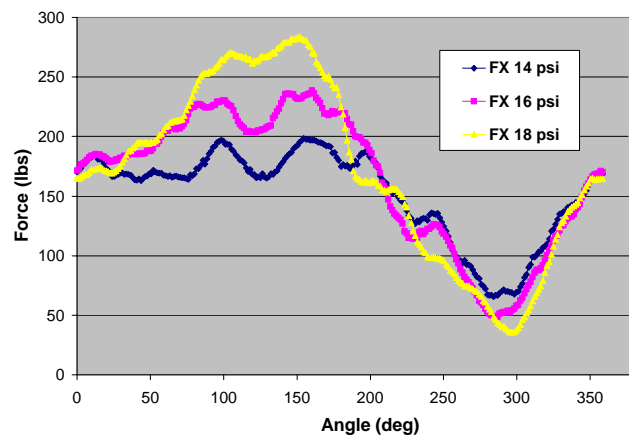


**Figure 7b. Blade thrust, Fx w/o DC correction**

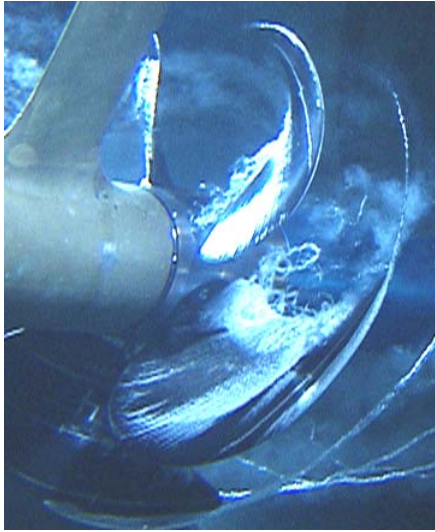


Figure 8a.  $J=1.12$ , 1698 rpm, 14 psi,  $\sigma=1.16$



Figure 8b. 18 psi,  $\sigma=1.5$

### 7.1 Bias Correction on Blade Thrust

To better quantify the periodic thrust loads, a bias correction was made to the  $F_x$  measurements. In Figure 7b the Alternating/Mean values w/o cavitation were about 0.72. This was significantly larger than the expected value of 0.4. This was thought to be due to a DC offset in the thrust level due to the dynamometer clamping bias mentioned earlier. The conventional shaft dynamometer was useable in this configuration, (even with the slip ring assembly) to measure overall thrust and torque. The comparison of the shaft thrust to the measured mean  $F_x$  force is shown in Figure 9 as a relatively constant shift in thrust over the range of operating ahead conditions investigated,  $J_a=1.1-1.3$ . With the consistency of the trend, it was reasonable to make a DC type mean bias error correction to the  $F_x$

force data. The alternating force levels were assumed correct, and the mean force was corrected to match the levels produced by the standard shaft dynamometer. When the correction was made to the measured blade thrust, shown in Figure 10, the data compared well to prediction made to MPUF3A (2005) computations using wake survey data as shown in Figure 6. This provided sufficient validity in the thrust and spindle torque data to provide quantitative observation on effects of cavitation.

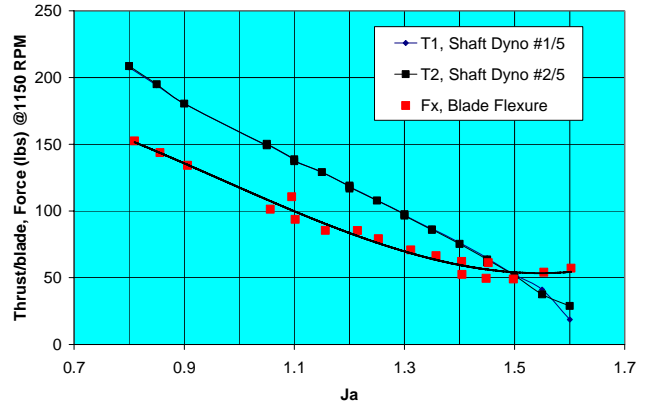


Figure 9. Comparison of Shaft thrust and blade thrust w/flexure at 1150 rpm

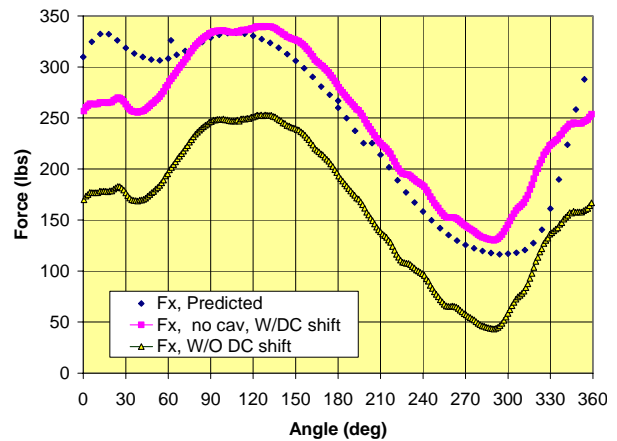


Figure 10. Alternating thrust,  $F_x$ , w/ and w/o bias correction,  $J=1.17$ , 1621 rpm, no cavitation

### 7.2 Bin Averaged Alternating / Mean Loads

The ratio of alternating to mean loads is the primary metric for evaluating the unsteady loads on controllable pitch propellers. A ratio of around 0.4 was shown in Figure 11 for P4990 operating at  $J=1.12$ . This would be a typical value for operation at design full power conditions at typical shaft configurations. For this case the flow inclination is 8.9 degrees.

An attempt was made to quantify the effects of cavitation by noting the maximum and minimum thrust levels in Figure 11 and plotting versus the cavitation number,  $\sigma$  ( $\sigma = (P - P_v) / 0.5\rho V^2$ ), along with the  $K_t$  levels measured with the shaft dynamometer, indicating thrust breakdown, shown in Figure 12. At the start of breakdown, the alternating blade thrust levels increase

about 10%, then decrease about 35% due to extensive cavitation. The increase in alternating load can be attributed to the moderate leading edge cavitation seen in Figure 8b.

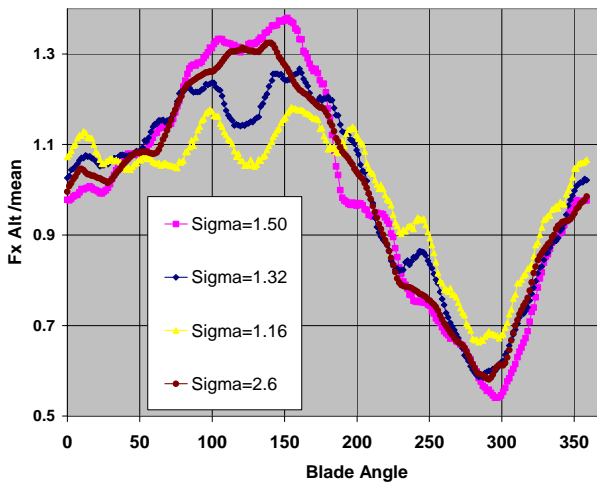


Figure 11. Alt/mean blade thrust, w/ DC correction,  $J=1.12$

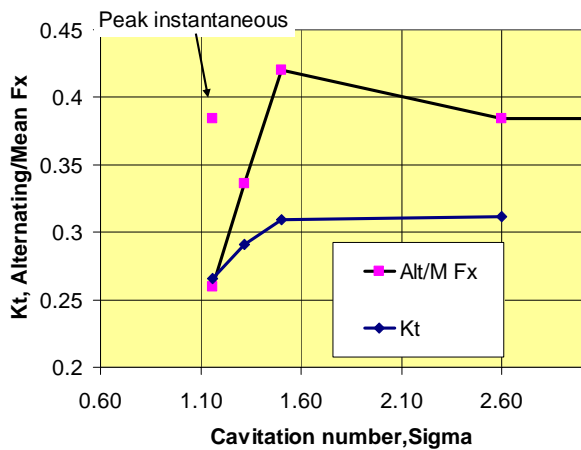


Figure 12. Change in alternating to mean thrust loading with cavitation breakdown,  $J=1.12$

### 7.3 Bin Averaged RMS Force Levels

By bin averaging the data by blade angular position, rms force levels can be correlated to cavitating and noncavitating unsteady blade force sources. Figure 13 shows a noncavitating case highlighting the loading when the blade passes through the strut and shaft wakes. Just prior to the blade center axis intersecting the strut wake center, a peak in the rms level of the blade thrust can be seen, a second peak corresponds to the wake of the shaft and the third peak, the second strut. These peaks are shifted in angle due to the leading ledge of the blade precessing well ahead of the blade center axis, by 5-30 degrees, depending on radial location. In the low turbulence regions of the flow field, the fluctuating component of thrust is around 2%. This is reasonable, since the turbulence level in the tunnel has been measured to be about 1.5%, and it has been noted that these propellers even at these test speeds have shown some laminar blade flow at intermediate radii.

Under cavitating conditions the bin averaged rms levels increase significantly, as expected. Figure 14 shows the propeller blade thrust variation with increasing cavitation as cavitation number is reduced. The fluctuation associated with the shaft and strut wake becomes dominated by the growth and collapse of the cavitation. A local peak can be seen around 75 degrees, which could be associated with the local steep gradient in load with angle or the initiation of leading edge cavitation.

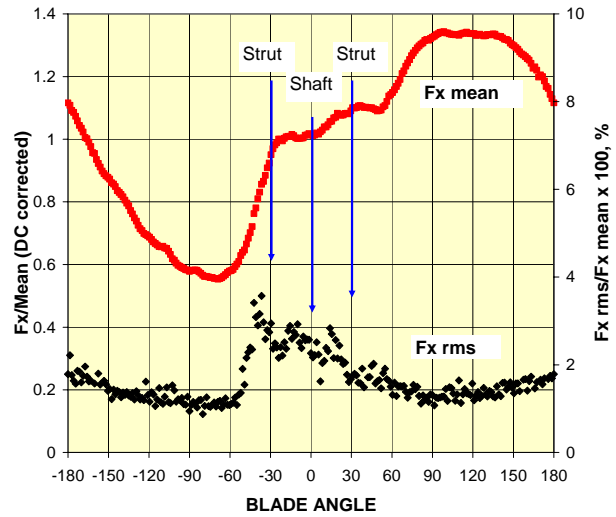


Figure 13. Bin average rms blade thrust levels under non-cavitating conditions

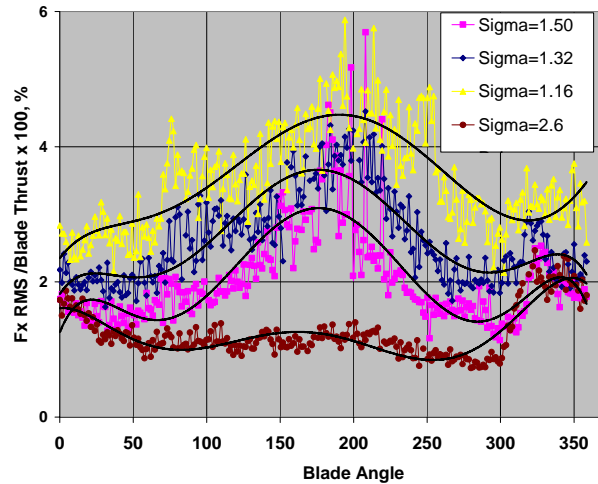


Figure 14. Bin average rms blade thrust levels under cavitating conditions

Figure 15 shows the bin averaged, rms and total 20,000 point accumulation of data to show a more complete picture of the load data in the stationary nonfrequency domain. There still is no clear explanation of the periodic bin averaged nature of the blade thrust, which appears to oscillate from 50 to 200 degree blade position at  $\sigma = 1.16$ . Observations of the videos show some tendency towards periodic cavity oscillation,

but there is no obvious cavity fluctuation. Relative to the cavity collapse phase, seen in Figure 14 at around 200 and 250 degrees at  $\sigma=1.16$ , and around 180 degrees at  $\sigma=1.5$ , a large increase in rms levels correspond to locations of cavity collapse from the videos and locations of decreasing  $F_x$  with blade angle.

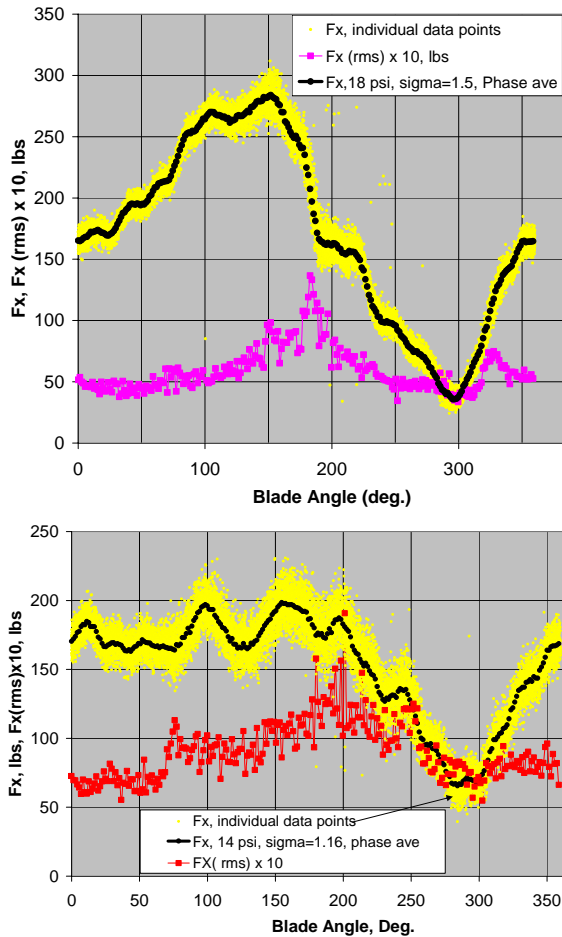


Figure 15. Phase average mean, rms, and all accumulated measured data

### 7.4 Transient Force Record Analysis

To further investigate the nature of the observed loading with effects of cavitation, individual record analysis was performed. This permits observation of extreme loading events, and may help explain the bin averaged periodicity in the bin averaged loading.

First, the resonant dynamic response of the blade, including the attached dynamometer was determined by performing tapping tests in water. The spectral analysis of the three loading channels is shown in Figure 16.

Resonances were determined and the associated cycle periods were computed in Table 3. The first mode of the dynamometer/blade dynamic system was at 178 Hz corresponding to cycle period of 55-57 degrees covering the conditions discussed. This period corresponds to the large amplitude oscillation seen when cavitation occurred primarily around 70 to 200 degrees. Interestingly, if blade vibration contributed to the vibratory response, it phase locked to the initiation of

cavitation at the same angular position for each revolution.

To look at extreme events, from Figure 14 at  $\sigma=1.16$ , the extreme individual data sample at 107 degrees was identified in the excel file from the plot. The  $F_x$  data verses angle associated with that revolution were plotted, shown in Figure 17. The extreme load event is clearly identified with oscillations occurring with a period of 20 degrees which corresponds to the 496 Hz resonance of the dynamometer/blade mechanical system.

Figure 18 shows the same individual sample record for the spindle torque,  $M_y$ . Phase locked vibrations occur at 350 Hz, the second resonant harmonic, at a period of around 30 degrees. The tap test shows a larger response for  $M_y$  at 348 Hz, the fundamental mode, but that result is likely dependent on where the blade was taped, which could not be carefully controlled during the tap test. Also to note is the clear effect of the cavity collapse phase, which is more pronounced for  $M_y$  than seen on thrust,  $F_x$ . Large rms levels and instantaneous fluctuations are seen around 210-250 degrees, where the sheet cavitation collapses. This is expected due to the wide blades and the collapse at the trailing edge inducing a large spindle moment.

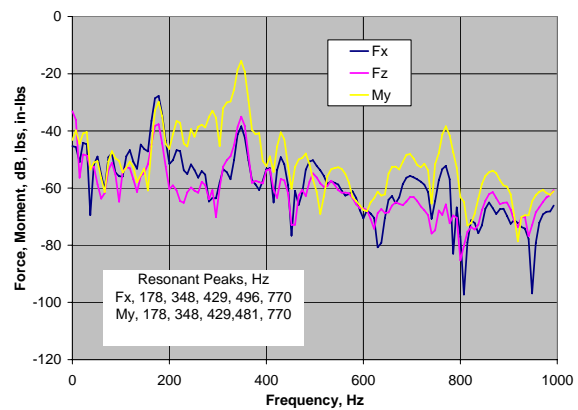


Figure 16. Spectra of tap test in water

Table 3. Resonant frequencies and blade angle periods

rpm	rps	res freq	angle (deg)/period
1621	27.02	178	55
1621	27.02	348	28
1621	27.02	429	23
1621	27.02	496	20
1621	27.02	770	13
1698	28.30	178	57
1698	28.30	348	29
1698	28.30	429	24
1698	28.30	496	21
1698	28.30	770	13

### 7.5 Discussion of cavitation effects on blade vibration and loads

The previous discussion of the test results leads to conclude that the transient cavitation has significant effects on the blade/hub vibratory response, which influences the measured loads. It was thought that these effects would be somewhat random in nature, and would phase average out of the resultant periodic loading. This

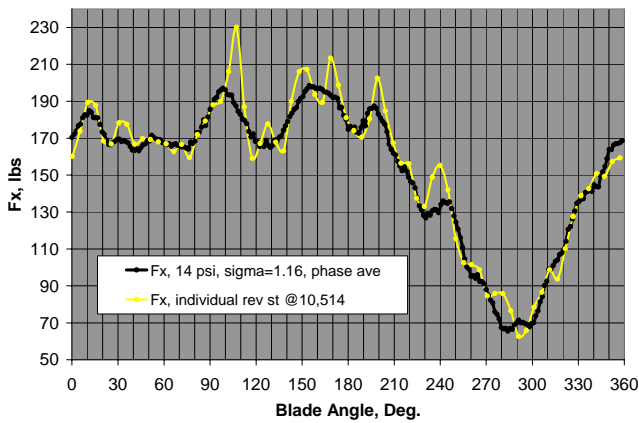


Figure 17. Individual Fx extreme record

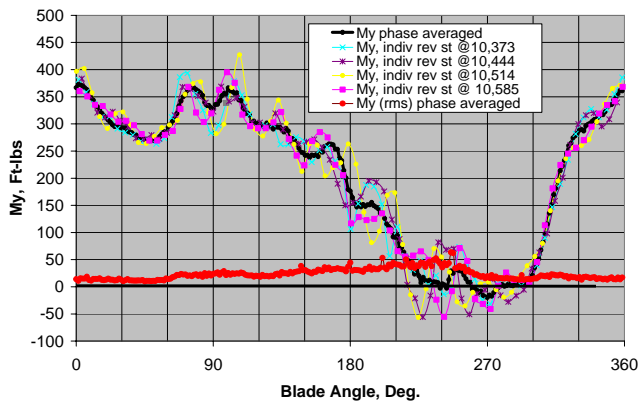


Figure 18. Individual spindle torque, My sample record, sigma=1.16

was not the case for the lower resonant harmonics. The onset of cavitation on the same angular position for each revolution provided a consistent impulse to the blade, which excited it periodically to vibrate. The higher harmonics (496 Hz for Fx) did phase average out, but contributed to the instantaneous peak loads. The peak loads for the sigma=1.16 case were extracted from the data in Figure 14, and plotted on Figure 17. Ironically, it shows that when considering the transient peak loads, the reduction in alternating to mean loading due to cavitation is returned back to the noncavitating case, such that the assumption of using the noncavitating loads for design is not unreasonable.

The real issue is how this applies to full scale. Do full scale controllable pitch propeller components have similar scaled stiffness as the model scale dynamometer? Simple full scale resonance checks could determine how the blade/hub mechanical system would respond to the high impacts of cavitation that the model scale propeller appeared to see.

## 8 Comparison of measured and predicted loads

MPUF3A was used to predict the periodic blade thrust, Fx, and spindle torque, My, and compare to the measured water tunnel results. The wake survey from Jessup (1993) was used with some refinement made to the shaft wake based on an LDV survey conducted recently. Figure 19 compares the blade thrust, Fx. It should be noted that the measured mean was matched to the measured shaft dynamometer measurement. For the noncavitating case, the alternating thrust matches well, except in the region of the shaft wake, where the predicted thrust is high, indicating the assumed wake would be lower than actual. At sigma=1.16, under extreme cavitating conditions, the alternating levels are also predicted a little low, but are also high in the shaft wake region. The measured oscillatory loading seen from 30-180 degrees is not seen in the calculations, a further indication of vibratory effects, not captured in the computations.

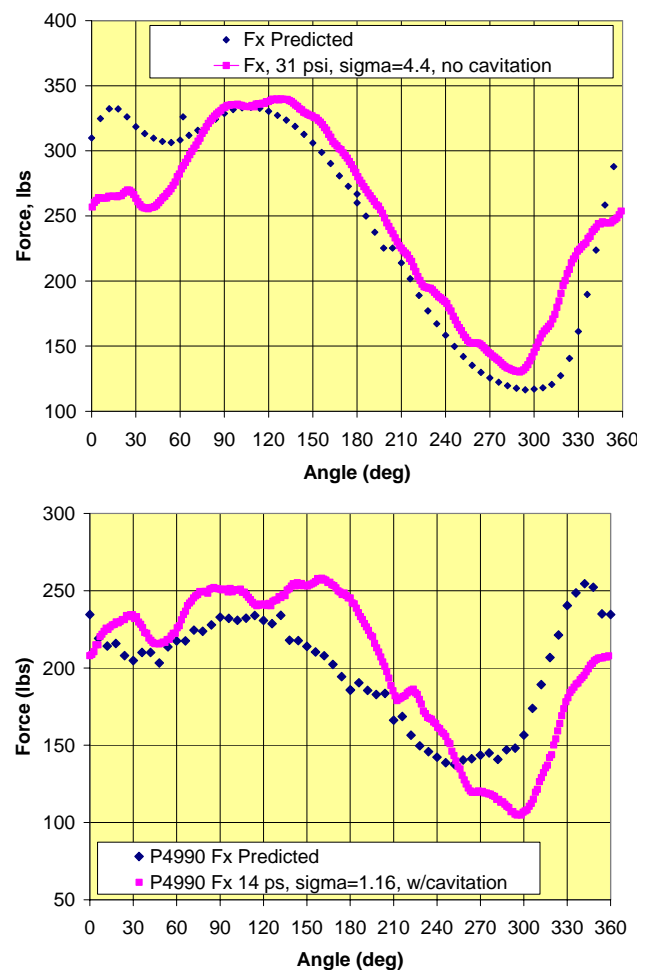


Figure 19. Propeller 4990 computed Fx w/ MPUF3A at 1621 rpm, Ja=1.17 w/ and w/o cavitation

The comparisons of My are shown in Figure 20. For the noncavitating case, a very good match is seen at the intermediate and lower loading angular positions. At the high loading conditions, from 330 to 150 degrees, the predictions are low. This is due to under prediction of the

chordwise loading at higher angles of attack. With cavitation, this effect is more pronounced.

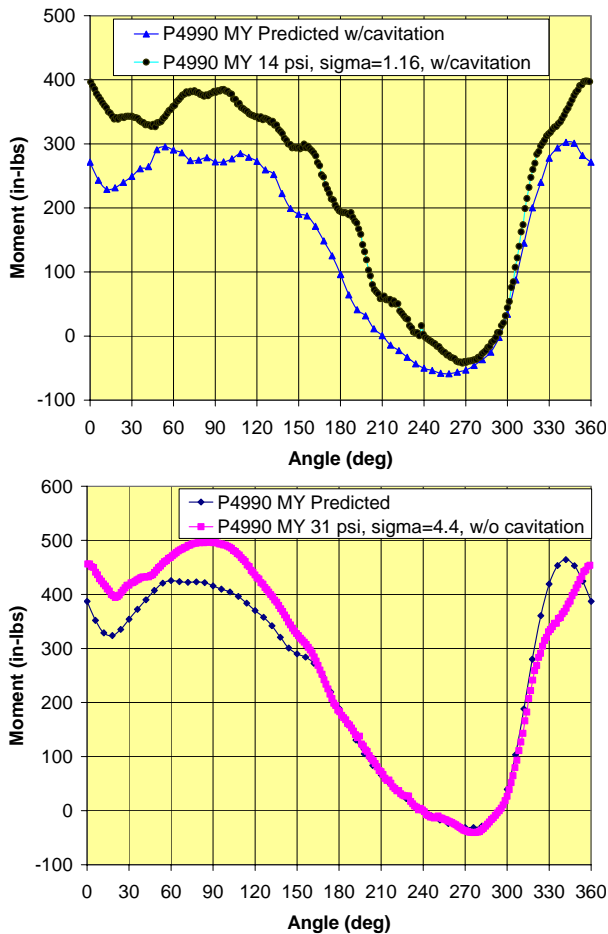


Figure 20. Propeller 4990 computed  $M_y$  w/ MPUF3A at 1621 rpm,  $J_a=1.17$  w/ and w/o cavitation

## 9 CONCLUSIONS

A pioneering set of model propeller load measurements were performed incorporating an in-hub blade dynamometer, and a downstream slip ring assembly to document effects of cavitation on periodic propeller blade loads. The experiment was a single attempt effort, which required in situ calibrations, and post test bias corrections to arrive at some fundamental conclusions about effects of cavitation on blades loads.

1. For propellers operating with extensive cavitation, which result in thrust breakdown, the alternating/mean loading, which typically is about 40% for a conventional open shaft and strut configuration, is reduced up to 35% depending on the degree of thrust breakdown (see Figure 12).
2. CP propeller blade and hub systems should be considered as dynamical systems which could be adversely excited by cavitation. The vibration induced by cavitation can return the instantaneous alternating /mean load levels back to the noncaviting values. This was demonstrated at model scale.
3. The prediction code, MPUF3A has shown the ability to capture the trends in the effects of cavitation. A more apparent modelling error can be seen in spindle torque.

## 10 ACKNOWLEDGEMENTS

The authors would like to acknowledge the contributions of Mr. James Bailar, for performing the MPUF3 calculations. Also, we express thanks to Dave Burroughs and Richard Suber for assisting in rigging and assembly of the water tunnel hardware.

## 11 REFERENCES

- Boswell R.J., S.D. Jessup And J.J. Nelka, (1978) "Experimental Unsteady And Time-Average Loads On The Blades Of A Cp Propeller Behind A Model Of The DD 963," SNAME Propeller Symposium, Virginia Beach, VA.
- Fuhs, D., (2005) "Evaluation of Propeller Unsteady Force Codes for Noncavating Conditions," NSWCCD-50-TR-2005/004.
- Jessup, S.D., K.D. Remmers, and W.G. Berberich, (1993) "Comparative Cavitation Evaluation of a Naval Surface Ship Propeller," ASME Int. Symposium on Cavitation Inception, FED-Vol. 17710, New Orleans, LA, December.
- Kinnas, S.A., J.-K. Choi, H. S. Lee, Y.L. Young, H. Gu, K. Kakar, and S. Natarajan, (2002) "Prediction of Cavitation Performance of Single/Multi-Component Propulsors and Their Interaction with the Hull," Trans. SNAME.